Mol Cell Proteomics Papers in Press. Published on September 19, 2018 as Manuscript RA118.000880

A new tool to reveal bacterial signaling mechanisms in antibiotic treatment and resistance

Miao-Hsia Lin[1,2], Clement M. Potel[1,2], Kamaleddin Haj Mohammad Ebrahim Tehrani[3], Albert J. R. Heck[1,2], Nathaniel I. Martin[3], Simone Lemeer[1,2 #]

1. Biomolecular Mass Spectrometry and Proteomics, Bijvoet Center for Biomolecular Research and Utrecht Institute for Pharmaceutical Sciences, University of Utrecht, Utrecht, The Netherlands

2. Netherlands Proteomics Center, Utrecht, The Netherlands

3. Department of Chemical Biology & Drug Discovery, Utrecht Institute for Pharmaceutical Sciences, University of Utrecht, Utrecht, The Netherlands

#Correspondence to: Simone Lemeer, s.m.lemeer@uu.nl
Postal address:
Biomolecular Mass Spectrometry and Proteomics
Utrecht University
Padualaan 8
3584 CA, Utrecht, the Netherlands
Phone: +31-2539974

Abbreviations

AMR	Antimicrobial resistance
IMAC	Immobilized metal ion affinity chromatography
mcr-1	Mobilized colistin resistance gene
MIC	Minimal inhibitory concentration
LB	Luria-Bertani
LC	Liquid chromatography
HCD	Higher energy collision induced dissociation
FDR	False discovery rate
GO	Gene ontology
pEtN	Phosphoethanolamine
pEtN trans	Phosphoethanolamine transferase
PCA	Principle component analysis
HTH	helix-turn-helix
TCEP	tris(2-carboxyethyl)phosphine
CAA	2-chloroacetamide
SDC	Sodium deoxycholate

Abstract

The rapid emergence of antimicrobial resistance is a major threat to human health. Antibiotics modulate a wide range of biological processes in bacteria and as such, the study of bacterial cellular signaling could aid the development of urgently needed new antibiotic agents. Due to the advances in bacterial phosphoproteomics, such a system-wide analysis of bacterial signaling in response to antibiotics has recently become feasible. Here we present a dynamic view of differential protein phosphorylation upon antibiotic treatment and antibiotic resistance. Most strikingly, differential phosphorylation was observed on highly conserved residues of resistance regulating transcription factors, implying a previously unanticipated role of phosphorylation mediated regulation. Using the comprehensive phosphoproteomics data presented here as a resource, future research can now focus on deciphering the precise signaling mechanisms contributing to resistance, eventually leading to alternative strategies to combat antimicrobial resistance.

Introduction

Antimicrobial resistance (AMR) has become one of the most serious threats to global health. At the rate at which resistance against antibiotics is currently rising it is not inconceivable that we will be confronted with a situation in which the actual last resort antibiotics become ineffective. It is estimated that AMR could cause 10 million deaths every year by the year 2050 (1) . In order to effectively combat the threat of AMR, understanding of the molecular mechanisms underlying resistance acquisition is essential.

The noun antibiotic, first described in 1941 by Selman Waksman, represents any small molecule made by a microbe that inhibits the growth of other microbes (2), but an alternative view of antibiotics envisions them as signaling molecules (3-5). The antibiotic colistin is a cationic cyclic decapeptide with a lipophilic fatty acyl side chain which is used as a last resort antibiotic for the treatment of multidrug resistant Gram negative infections (6). Alarmingly, a plasmid-mediated colistin resistance mechanism (*mcr-1* gene) has been reported in over 30 countries across five continents since it was first identified in 2015, raising major public health concern (7-9). Ciprofloxacin is another critically important antimicrobial with possible serious side effects (10) used to treat infections resistant to safer antibiotics. Ciprofloxacin is one of the most commonly prescribed fluoroquinolones in current medical practice and its resistance rate has raised from 1.8 to 15.9 % over only 10 years (11). Overall, the worldwide spread of AMR in recent years is a sobering reminder of our need to better understand resistance mechanisms in order to design new effective inhibitors.

While the characterization of resistance genes was already made possible by advances in functional metagenomic approaches, these methods cannot quantify proteins and decipher the potential bacterial signaling cascades involved in AMR. The study of bacterial cellular signaling in AMR

and AMR acquisition could thus provide opportunities for the development of new therapeutic strategies. Bacteria are capable of modifying serine/threonine/tyrosine residues on proteins like eukaryotes, but in addition use two-component signaling which relies on histidine autophosphorylation of sensory kinases as the first component and aspartate phosphorylation of response regulators as the second component (12). Reversible protein phosphorylation is a well-established mechanism of regulating gene expression in response to a variety of environmental stress factors (13) and in recent years, growing evidence has linked two-component systems as well as Serine/Threonine/Tyrosine kinase signaling to AMR (13-15). While mass spectrometry-based proteomics has enabled the study of signaling dynamics on a global scale through the quantification of site-specific protein phosphorylation in eukaryotes, the study of bacterial phospho-signaling has largely lagged behind due to technical hurdles. Our recent developments in this area enable us to reach in-depth coverage of bacterial phosphoproteomes (16, 17), offering the unprecedented opportunity to study signaling mechanisms during antibiotic treatment, resistance acquisition and full resistance.

Here we set out to detect changes in proteome and phosphoproteome of antibiotic treated bacteria in order to detect regulated expression and signaling which correlates with antibiotic susceptibility. To this end we treated *E. coli* with increasing doses of ciprofloxacin or colistin for several days, in order to decrease the susceptibility to the antibiotic. In the case of colistin, we also analyzed the (phospho)proteome of a *bona fide*, clinically isolated colistin resistant *E. coli* strain carrying the mcr-1 plasmid. Our results indicate that antibiotic susceptibility rapidly increases for ciprofloxacin treatment, coinciding with extensive changes in phosphoproteome. For short-term colistin treatment, changes in phosphoproteome resemble the phosphoproteome of the *bona fide mcr-1*

positive strain, despite the lack of a clear resistant phenotype, indicating that changes in signaling precede resistance development.

Materials and Methods

Bacterial strains. Two *Escherichia coli* strains were used in this study: the wild-type *E. coli* strain W3110 (CGSC, Coli Genetic Stock Center) and one clinically isolated *mcr-1* positive strain which carries the *mcr-1* gene containing plasmid, conferring colistin resistance as the minimal inhibitory concentration (MIC) was 8 µg/mL (experimentally determined). This strain was isolated as part of routine diagnostic procedures in the University Medical Center Utrecht (Utrecht, the Netherlands) from a blood culture. This aspect of the study did not require consent or ethical approval by an institutional review board. The MIC of ciprofloxacin or colistin was determined by the dilution method in microtiter plates as previously described (18). For the *E. coli* W3110 wild-type strain, the MIC for colistin and ciprofloxacin was experimentally determined as 0.5 µg/ml and 16 ng/ml, respectively.

Resistance induction and bacterial cell collections. An overnight culture of wild-type *E. coli* strain was diluted 1:100 into Luria-Bertani (LB) medium with or without 4 ng/mL ciprofloxacin, representing ¼ the MIC of ciprofloxacin. After 24 h of incubation at 37 °C with shaking, the MIC was determined again. This same procedure was repeated until the MIC of ciprofloxacin increased to 128 ng/mL (3 days) and 1024 ng/mL (7 days) which are 8- and 64-fold higher than the original MIC. The same approach was used for colistin in which the wild-type *E. coli* cells were culture with LB medium with ¼ the MIC of colistin. However, no MIC increase was detected after 4 days up to 10 days of treatment. In order to detect the early response to colistin, phosphoproteome analysis was further performed on the 4 day treated *E. coli*. For all (phospho)proteomic analysis, 1 ml of culture was transferred 100 ml culture medium including antibiotics. *E. coli* was subsequently grown to early-stationary phase (OD_{600}=1.2) after which samples for proteome and phosphoproteome analyses were collected. Briefly, bacterial cells

were collected by centrifugation at 3000 *g* at 4 °C for 15 minutes. The cell pellets were washed twice with ice-cold PBS and stored at -80 °C until further processes.

Cell lysis and protein extraction. All different *E. coli* cells with varied MICs to ciprofloxacin or colistin were lysed as described previously (16, 17). Briefly, cell pellets were resuspended with lysis buffer (100mM Tris-HCl pH 8.5, 7 M Urea, 1% SDC (Sigma-Aldrich), 5 mM TCEP, 30 mM CAA, 10 U/ml DNase I, 1 mM magnesium chloride (Sigma Aldrich), 1% benzonase (Merck Millipore), phosphoSTOP (Roche) and complete mini EDTA free (Roche)) and lyzed by sonication for 45 minutes (20 seconds on, 40 seconds off) using a Bioruptor Plus. Cell debris was removed by ultracentrifugation (140 000g for 1h at 4°C). 1% benzonase was added to the supernatant and the mixture was incubated at room temperature for 2h. Protein concentration was determined by a Bradford protein assay (Bio-Rad) using bovine serum albumin (BSA) as the protein standard. Impurities were removed by methanol/chloroform protein precipitation as follows: 1 mL of supernatant was mixed with 4 mL of methanol (Sigma-Aldrich), 1 mL chloroform (Sigma-Aldrich) and 3 mL ultrapure water with thorough vortexing after each addition. The mixture was then centrifuged for 10 min at 5,000 rpm at room temperature (RT). The upper layer was discarded and 3 mL of methanol was added. After sonication and centrifugation (5,000 rpm, 10 min at RT), the solvent was removed and the precipitate was allowed to air dry. The pellet was resuspended in a buffer composed of 100 mM Tris-HCl pH 8.5, 1% SDC, 5 mM TCEP and 30 mM CAA. Trypsin (Sigma-Aldrich) and Lys-C (Wako) proteases were respectively added to a 1:25 and 1:100 ratio (w/w) and protein digestion was performed overnight at RT.

Peptide desalting. The tryptic peptide mixtures were acidified to pH 3.5 with 10 % formic acid (Sigma-Aldrich) and centrifuged at 14000 rpm for 10 minutes at 4 °C. The supernatant was then loaded on a 200 mg (3cc) tC18 Sep-Pak resin (Waters), washed with 2x1 mL of 0.1% formic acid

and peptides were eluted with 30% acetonitrile (Sigma). Eluted peptides were subsequently dried down using a lyophilizer and subjected to proteome analysis or phosphopeptide enrichment.

Fe^{3+}-IMAC phosphopeptide enrichment. Enrichments were performed as previously described(17). Briefly, lyophilized peptides were dissolved in buffer containing 30% acetonitrile and 0.07% trifluoroacetic acid (TFA, Sigma-Aldrich)) and the pH was adjusted to a value of 2.3 using 10% TFA prior to injection onto the Fe^{3+}-IMAC column (Propac IMAC-10 4 x 50 mm column, Thermofisher scientific). The elution buffer is composed of 0.3% NH_4OH. UV-abs signal was recorded at the outlet of the column, at a wavelength of 280 nm. Collected phosphopeptides were immediately frozen in liquid nitrogen and subsequently dried down using a lyophilizer.

LC-MS/MS. Nanoflow LC-MS/MS analysis was performed by coupling an Agilent 1290 (Agilent technologies, Middelburg, Netherlands) to an Orbitrap Q- Exactive HF (Thermo Scientific, Bremen, Germany). Lyophilized peptides were dissolved in loading buffer (10% FA in the case of proteome samples and 20 mM citric acid (Sigma-Aldrich) complemented with 1% formic acid in the case of phosphoproteome samples) and injected, trapped and washed on a pre-column (100 µm i.d. × 2 cm, packed with 3 µm C18 resin, Reprosil PUR AQ, Dr. Maisch, packed in-house) for 5 minutes at a flow rate of 5 µL/minute with 100 % buffer A (0.1 % FA, in HPLC grade water). Peptides were then transferred to an analytical column (75 µm x 60 cm Poroshell 120 EC-C18, 2.7 µm, Agilent Technology, packed in-house) prior to separation at room temperature at a flow rate of 300 nL/min using a 115 minutes linear gradient, from 13% to 44% buffer B (0.1 % FA, 80 % ACN). Electrospray ionization was performed using 1.9 kV spray voltage and a capillary temperature of 320 °C. The mass spectrometer was operated in data-dependent acquisition mode: full scan MS spectra (m/z 375 – 1,600) were acquired in the Orbitrap at 60,000 resolution for a maximum injection time of 20 ms with an AGC target value of $3e^6$. Up to 12 precursors were

selected for subsequent fragmentation and high-resolution HCD MS2 spectra were generated using a normalized collision energy of 27 %. The intensity threshold to trigger MS2 spectra was set to $2e^5$, and the dynamic exclusion to 15 seconds. MS2 scans were acquired in the Orbitrap mass analyzer at a resolution of 30,000 (isolation window of 1.4 Th) with an AGC target value of $1e^5$ charges and a maximum ion injection time of 50 ms. Precursor ions with unassigned charge state as well as charge state of 1+ or superior/equal to 6+ were excluded from fragmentation.

Data Analysis. MaxQuant software (version 1.6.0.1) was used to process the raw data files, which were searched against the database merging reviewed *E*. coli K12 sequences (*E.coli* K12 Uniprot database, March 2016, 4434 entries) and *mcr-1* strain sequences (5005 entries) and removing duplicates, with the following parameters: trypsin digestion (cleavage after lysine and arginine residues, even when followed by proline) with a maximum of 3 missed cleavages, fixed carbamidomethylation of cysteine residues and variable modifications of methionine oxidation and Protein N-terminal acetylation (19). In case of phosphoproteome analysis, the variable modification of phosphorylation on serine, threonine, tyrosine, histidine, and aspartate residues was also included. Mass tolerance was set to 4.5 ppm at the MS1 level and 20 ppm at the MS2 level. The False Discovery Rate (FDR) was set to 1% at the peptide and protein level, an additional peptide score cut-off of 40 was used for modified peptides and the minimum peptide length was set to 7 residues. In terms of label-free quantification analysis, the match between runs (MBR) function was used with the retention time window of 1 minutes. The MaxQuant output tables "evidence.txt" and "phospho (HDSTY)Sites.txt" from phosphoproteome dataset and "proteinGroups.txt" from proteome datasets were further used to calculate the identification number of unique phosphopeptides, phosphosites, and proteins. The table of phospho (HDSTY)Sites.txt and "proteinGroups.txt" were further used for quantification analysis at

phosphoproteome and proteome level, respectively, using Perseus (version 1.6.0.2) (20). Known contaminants as provided by MaxQuant and identified in the samples were excluded from the analysis. The list of modified peptides was further filtered at the level of phospho-site localization using a localization probability threshold of 0.75 to derive all class I phospho-sites. To determine phosphorylation sites corresponding to dynamic profiles due to changes in phosphorylation state rather than protein abundance, we normalized the phosphosite level by the corresponding changes in protein abundance. To detect the complete matrix of intensities for on/off regulation in quantification analysis, missing value imputation was performed when all 3 values existed in at least on condition. The log2 scale of phosphosites or proteins intensity were subjected into a two-way ANOVA test with a false discovery rate (FDR) of less than 0.05.

Bioinformatic analysis. The Gene Ontology analysis was performed with PANTHER (http://www.pantherdb.org/), with p-value < 0.05. The KEGG pathway enrichment was performed using ClueGO app in Cytoscape (version 3.5.1) with the p-value <0.05(21). Phosphorylation motifs were analyzed using the Motif- algorithm with occurrences set to 10 and significance set to 0.00001, using the whole genome sequence as background (22). Sequence logos were generated by iceLogo (23). For protein sequence alignment, full-length protein sequences were aligned using the Clustal X program with default settings and after alignment, phosphosite regions were displayed. All protein sequences from the same gene in different gram-negative bacteria, relatively close to *E. coli*., were download from Uniprot.

Experiment design and statistical rationale. Each sample was enriched in triplicate before being injected separately into the LC-MS/MS system. Each raw file was separately processed using the MaxQuant software. Triplicate analysis was sufficient to saturate the number of phosphosites detected.

Results

Proteome profiling demonstrates differential protein expression triggered by continuous exposure to antibiotics

Wild-type *E. coli* cells were continuously exposed to low dosage, corresponding to one-quarter of the Minimum Inhibitory Concentration (MIC), of either colistin or ciprofloxacin to decrease the antibiotic susceptibility and trigger AMR (Fig. 1A). For ciprofloxacin we indeed observed a rapid increase in MIC, resulting in a 8-fold higher MIC after 3 days and a 64-fold higher MIC after 7 days (Fig. 1a). For colistin we did not observe a higher MIC after 4 days nor at 10 days of treatment, indicating a clear difference in response to the antibiotics used (Fig 1A, Supplementary Fig 1A). To comprehensively survey cellular signaling at early stages of antibiotic treatment and early resistance development, label-free quantification of both proteome and phosphoproteome was performed (Supplementary Fig. 1). Due to the lack of a clear resistant phenotype at 10 days of colistin treatment, we focused our (phospho)proteome analysis to the 4 day time point, in order to get insight into the early onset effects of colistin treatment. At a false discovery rate (FDR) of 1% at the protein level, this resulted in the identification of 2,850 proteins (Supplementary Table 1), from which 2,567 were quantified, achieving a similar coverage as previous *E. coli* proteome studies, but within a significant shorter analysis time (24). Moreover, similar Gene Ontology (GO) profiles were obtained at the proteome and genome levels, confirming the completeness of our proteome coverage (Supplementary Fig. 2). We next evaluated these protein expression patterns to detect differential expression related to antibiotic treatment and resistance. Principle component analysis of colistin and ciprofloxacin proteome data clearly segregated samples into three groups. Furthermore the analysis indicated that the serially-passaged *E. coli* treated with low dose of colistin are closer related to *mcr-1*-positive cells than to untreated cells, despite the lack

of a clear resistant phenotype in serially passaged colistin treated *E.coli* (Fig. 1A and 1B). As expected, the phosphoethanolamine (pEtN) transferase coded by *mcr-1* (pEtN trans) was only identified in the *mcr-1* clinical strain (Fig 1C). Surprisingly, several classes of proteins known to be involved in resistance exhibited significant changes in expression upon colistin treatment as well as in the *mcr-1* cells. The multidrug efflux pump (AcrA) as well as a variety of proteins involved in cell wall biogenesis, such as the Bam protein complex (25), LPS assembly outer membrane protein LptE (26), and the peptidoglycan biosynthesis proteins (MltA and MltB) (27) were more expressed in colistin serially-passaged as well as in *mcr-1* cells (Fig. 1c and Supplementary Table 2). Furthermore, the glycolysis/gluconeogenesis pathway and protein translation were down regulated both treated and resistant cells, which is consistent with the concept of compensatory fitness cost in developing resistance (28, 29) (Fig. 1C and Supplementary Table 2).

For induced ciprofloxacin resistance, similar regulation patterns were observed, as expression levels of lipoproteins (n=22) or proteins involved in cell wall biogenesis (n=21) and cell cycle (n=19) were highly increased when antibiotic susceptibility decreased (Fig. 1D and Supplementary Table 2). In agreement with ciprofloxacin targeting DNA gyrase activity, a significant number DNA repair system proteins (n=21) were increasingly expressed when resistance developed (Fig. 1D and Supplementary Table 2). Compared to colistin, ciprofloxacin induced the expression of a different panel of multidrug efflux system proteins including MdtK, EmrA, SbmA, and MdlA proteins, which can be explained by the different nature of both antibiotics.

Bacterial protein phosphorylation is far more widespread than anticipated

Bacteria, as well as other organisms, have developed several phosphorylation dependent systems

to adapt to environmental stresses, including the well-known two-component system, which constitutes one of the most sensitive and efficient regulatory mechanisms in bacteria. To get detailed insight into differential phosphorylation associated with antibiotic treatment, changes in antibiotic susceptibility and resistance we subsequently profiled the phosphoproteomes of all samples (Supplementary Fig. 1). Our analysis resulted in the identification of 2,509 class I phosphosites (unambiguously localized) on 1,133 proteins (Supplementary Table 3). In contrast to commonly used phosphoproteomics workflows, which are usually based on the combination of fractionation and phosphopeptide enrichment (30, 31), all experiments here were performed in triplicate, which was sufficient to saturate the number of sites (Supplementary Fig. 3) with high quantification accuracy and reproducibility (Pearson correlation coefficient between 0.982 and 0.919, Supplementary Fig. 4). In total, we quantified 3,872 phosphopeptides, which span around four orders magnitude of peptide ion signal, allowing us to look beyond classically observed phosphorylations on high abundant metabolic enzymes (Fig. 2A). In fact, phosphorylation events on several transcription factors and those indicating kinase activity were identified in the lowest-abundance-range of the distribution We therefore hypothesized that the dynamics of phosphorylation signaling networks induced by antibiotics could be well profiled (Fig. 2A). The comprehensive and parallel measurements of phosphoproteome and proteome allowed us, for the first time, to investigate a possible correlation between a protein's abundance and its propensity to be phosphorylated. There is a weak but significant tendency between the number of identified phosphosites and increasing protein abundance (Fig. 2B, Pearson correlation as 0.65, $p < 0.01$) which is similar to the profile in the human phosphoproteome (32). About 45% of identified proteins were phosphorylated on just one residue, whereas the remaining 55% were phosphorylated at multiple sites (Fig. 2C). In addition, the GO term enrichment of identified

phosphorylated proteins correlates with the obtained proteome profile suggesting that we achieved a comprehensive phosphoproteome coverage (Supplementary Fig. 2). Moreover, the residue-specific phosphorylation pattern observed (Ser 56%, Thr 20%, Tyr 13%, Asp 5%, and His 5%; Fig. 2D) closely corresponds to previous published reports (33). When compared to the two existing databases, dbPSP and Uniprot, the work described here expands the known *E. coli* phosphoproteome by a factor 4 and as a result, 89.6 % of identified phosphosites (n=2248) were observed for the first time (Fig. 2E) (34). Overall, this work indicates that bacterial phosphorylation is far more widespread than anticipated, as 40% of the identified proteins are phosphorylated.

In-depth quantitative phosphoproteomics enables identification of potential regulators in resistance development

PCA analysis of the phosphoproteome data again segregated the *E. coli* cells according to antibiotic susceptibility (Fig. 3A, B). For ciprofloxacin, phosphoproteomes of 7 day treated cells were more distinct from the 3 days and non-treated treated cells. Surprisingly, for colistin, the 4 days treated cells resembled the resistant *mcr-1* cells, again despite the presence of a clear resistant phenotype, but in accordance with the proteome data. These results suggest that specific regulation at the phosphorylation level takes place upon antibiotics treatment, driving to a resistance-like phenotype (Fig. 3A). Indeed, a high percentage of identified phosphosites showed significant differential regulation during treatment and resistance: 460 phosphosites were significantly regulated in the colistin samples, while 911 were regulated upon ciprofloxacin treatment (ANOVA test, FDR< 0.05; Supplementary Table 4).

When looking closely at the significantly regulated phosphosites, we identified phosphorylation changes on several known resistance-related proteins. We observed increased phosphorylation of His717 on the ArcB sensor protein upon colistin treatment, a finding which is in agreement with previous studies showing that colistin stimulates the production of highly deleterious hydroxyl radicals, inducing high activity of the ArcAB two-component system as a resistance mechanism (35, 36). Phosphorylation levels of proteins involved in DNA transfer (relaxosome proteins : TraD, TraP) and integration host factor (IhfA)) (37), universal stress proteins (UspB and UspG) (38), Psp system (PspA and PspC) (39), and drug efflux proteins (OmpT) (40), were also regulated in the colistin serially-passaged *E. coli* (Fig. 3C and Supplementary Table 4).

Similarly, differential phosphorylation of known resistance-related proteins was observed upon ciprofloxacin treatment (Fig. 3D and Supplementary Table 4), for example on the DNA transfer-related proteins (TraM, IhfA, and IhfB), stress response proteins (UspA, UspF, and UspG) (38), psp system (PspA) (39), and the antibiotics degrading enzyme AmpC. Interestingly, phosphorylation of several DNA repair proteins (UvrA, UvrB, and UvrC) was significantly downregulated in ciprofloxacin resistant cells, implying that these phosphorylation events play a role in combating the effect of ciprofloxacin, which is a DNA gyrase inhibitor (Fig. 3D). ABC transporter and two-component system pathways, which are known to be related to evolution of resistance (14, 41), were significantly regulated in both colistin and ciprofloxacin treatments (Fig. 4). Though signal transduction *via* two-component systems is known to rely on reversible phosphorylation (12), regulated phosphosites identified here are mostly unknown, suggesting that the detailed signaling mechanisms underlying response and resistance to antibiotics are currently underestimated.

Furthermore, we identify for the first time enriched phosphorylation motifs in different regulatory clusters, implying that specific kinase/phosphatase systems are involved in antibiotic response and resistance (Fig. 3C, D). As an example, we observed the motif KxxS, matching to the HipA kinase's substrate motif, on Ser239 of the GltX protein. Interestingly, the HipA kinase was phosphorylated at both Ser150 and Asp146, albeit respectively up- and down-regulated during antibiotic treatment, suggesting that those two phosphosites may play a role in the regulation of the kinase function during resistance development (42). In addition, several specific tyrosine phosphorylation motifs were identified, suggesting the potential importance of tyrosine kinase-induced phosphorylation in resistance evolution (Fig. 3C, D). Protein phosphorylation occurring in the proximity of the protein N- or C-terminus was highly enriched, consistent with findings in a previous study (33). We here demonstrate the possible importance of these terminal phosphorylation events in resistance development (Fig. 3C, D). As such terminal phosphorylation events are possibly bacteria specific, the kinases responsible for these phosphorylations could represent adequate drug targets.

Regulated phosphosites involved in DNA transcription display evolutionary high conservation across bacterial species

Phosphorylation on DNA transcriptional regulators is of particular interest because of its potential to influence bacterial cell growth and pathogenicity (13). This spurred us to assess the residue conservation among regulated phosphosites identified on known transcription factors, as a high level of conservation can indicate conserved biological function (13). Amongst identified regulated phosphosites, several residues on winged helix-turn-helix (HTH) DNA binding domains were highly conserved in proteobacteria. This includes residues on the C-terminal effector domain

of the OmpR/PhoB subfamily transcription regulators such as Thr191, His200 and Ser202 residues on CpxR, Tyr194 on OmpR, and Ser214 and Tyr226 on BaeR (Fig. 5). Other evolutionary conserved phosphosites on HTH domains were observed at Thr141, Ser180, and Thr209 of Crp as well as on Thr2 of the AscG transcription regulator (Fig. 5). Our data thus suggest that protein phosphorylation in the HTH region might be a widespread mechanism of transcriptional control of genes implicated in antibiotic resistance.

Phosphosites identified on transcription regulators such as Tyr64 and Tyr 146 on RcsB, Ser282 on CysB, Ser3 on SlyA, Thr62, Thr126, Ser129, and Ser135 on YebC, and His230 on YeiE were also found to be highly conserved among bacterial orthologues (Supplementary Fig. 5). The observed upregulation of the conserved transcriptional regulatory protein RcsB phosphosites, Tyr64 and Tyr146, for colistin serially-passaged cells is consistent with previous reports establishing a link between the RcsCDB/F phospho-relay system and polymyxin resistance (43). In the same manner, high conservation of phosphorylated residues was found on other DNA binding proteins, including Hns, StpA, HupA, and HupB, in which regulated phosphosites located both on DNA binding or protein dimerization domains were found to be all highly conserved across bacteria (Fig. 6). Interestingly, the hns protein has been linked to multidrug resistance (44) and together with protein StpA coordinates OmpF porin gene expression and DNA conjugation in order to cope with environmental stress such as antibiotic administration (45, 46). In addition, histone-like proteins HupA and HupB are the most common bacterial DNA-binding proteins responsible for nucleoid compaction, therefore dynamic phosphorylation events located on DNA binding region and the N-terminal tail might be similar to eukaryotic histones phosphorylations and serve as sensors of cellular stress, ultimately leading to resistance-related gene expression (47). Therefore, the well-known eukaryotic histone-code may have a prokaryotic counter-part

Discussion

The concept that regulated protein phosphorylation in its various facets could contribute to defining new drug targets is not new *per se*. However, the thorough investigation of phosphorylation signaling pathways in bacteria has been mostly neglected. Here we present the broadest bacterial phosphorylation catalogue, representing 2509 phosphosites. Notably, the extent of phosphorylation regulation in bacteria is far more important than we anticipated and the fact that only 10.4% of identified phosphosites (n=261) are reported in the public databases, Uniprot and dbPSP, make this study a valuable resource for future, indispensable, work on deciphering signaling mechanisms involved in AMR.

We showed for the first time that specific phosphorylation motifs changed during resistance development. This is consistent with the idea that bacterial Ser/Thr/Tyr kinases are involved in resistance development (48), which has been proposed but never comprehensively studied. Moreover, regulated phosphorylation sites located on transcription factors and other DNA binding proteins showed high evolutionary conservation, indicating an important biological role. Finally, upon resistance development, we also observed specific regulation of N/C-terminal phosphorylation, which is unique to bacteria. Together, these regulated phosphorylation events during antibiotic treatment and resistance indicate that phosphorylation mediated signaling could be used as a specific target for drug design. In summary, we here describe the most comprehensive coverage of a bacterial phosphoproteome and monitor its dynamics upon perturbation by antibiotics. The unprecedented depth of our phospho-analysis, as well as the fact that significant reversible phosphorylation responses are observed upon antibiotic treatment opens up new avenues for research into novel alternative strategies to combat AMR. Future work should be aimed at understanding the contribution of each signaling pathway to resistance

development.

Acknowledgments

We acknowledge Willem van Schaik and Axel Janssen in providing the mcr-1+ strain and helpful discussions. S.L. acknowledges support from the Netherlands Organization for Scientific Research (NWO) through a VIDI grant (project 723.013.008). This work was supported by the Roadmap Initiative *Proteins@Work* funded by the Netherlands Organization for Scientific Research (NWO) (project number 184.032.201), and the MSMed program, funded by the European Union's Horizon 2020 Framework Programme to A.J.R.H. (grant agreement number 686547).

Author Contributions

M.H.L, C.M.P, K.H.M.E.T, N.I.M. and S.L. designed the experiment. M.H.L., C.M.P. and K.H.M.E.T performed the experiments. M.H.L., C.M.P., and S.L. performed data analysis. All authors contributed to the writing of the manuscript.

Competing financial interest

The authors declare no competing financial interest

Data availability

All raw data that support the findings of this study have been deposited in jPOST repository with the accession number as JPST000388.

References

1. O'Neill, J. (2016) Tackling drug-resistant infections globally: final report and recommendations https://amr-review.org/sites/default/files/160525_Final%20paper_with%20cover.pdf
2. Clardy, J., Fischbach, M. A., and Currie, C. R. (2009) The natural history of antibiotics. *Current biology : CB* 19, R437-441
3. Goh, E. B., Yim, G., Tsui, W., McClure, J., Surette, M. G., and Davies, J. (2002) Transcriptional modulation of bacterial gene expression by subinhibitory concentrations of antibiotics. *Proceedings of the National Academy of Sciences of the United States of America* 99, 17025-17030
4. Hoffman, L. R., D'Argenio, D. A., MacCoss, M. J., Zhang, Z., Jones, R. A., and Miller, S. I. (2005) Aminoglycoside antibiotics induce bacterial biofilm formation. *Nature* 436, 1171-1175
5. Yim, G., Wang, H. H., and Davies, J. (2007) Antibiotics as signalling molecules. *Philosophical transactions of the Royal Society of London. Series B, Biological sciences* 362, 1195-1200
6. Falagas, M. E., and Kasiakou, S. K. (2005) Colistin: the revival of polymyxins for the management of multidrug-resistant gram-negative bacterial infections. *Clinical infectious diseases : an official publication of the Infectious Diseases Society of America* 40, 1333-1341
7. Liu, Y. Y., Wang, Y., Walsh, T. R., Yi, L. X., Zhang, R., Spencer, J., Doi, Y., Tian, G., Dong, B., Huang, X., Yu, L. F., Gu, D., Ren, H., Chen, X., Lv, L., He, D., Zhou, H., Liang, Z., Liu, J. H., and Shen, J. (2016) Emergence of plasmid-mediated colistin resistance mechanism MCR-1 in animals and human beings in China: a microbiological and molecular biological study. *The Lancet. Infectious diseases* 16, 161-168
8. Wang, Y., Tian, G. B., Zhang, R., Shen, Y., Tyrrell, J. M., Huang, X., Zhou, H., Lei, L., Li, H. Y., Doi, Y., Fang, Y., Ren, H., Zhong, L. L., Shen, Z., Zeng, K. J., Wang, S., Liu, J. H., Wu, C., Walsh, T. R., and Shen, J. (2017) Prevalence, risk factors, outcomes, and molecular epidemiology of mcr-1-positive Enterobacteriaceae in patients and healthy adults from China: an epidemiological and clinical study. *The Lancet. Infectious diseases* 17, 390-399
9. Wang, R., van Dorp, L., Shaw, L. P., Bradley, P., Wang, Q., Wang, X., Jin, L., Zhang, Q., Liu, Y., Rieux, A., Dorai-Schneiders, T., Weinert, L. A., Iqbal, Z., Didelot, X., Wang, H., and Balloux, F. (2018) The global distribution and spread of the mobilized colistin resistance gene mcr-1. *Nature communications* 9, 1179
10. Fasugba, O., Gardner, A., Mitchell, B. G., and Mnatzaganian, G. (2015) Ciprofloxacin resistance in community- and hospital-acquired Escherichia coli urinary tract infections: a systematic review and meta-analysis of observational studies. *BMC infectious diseases* 15, 545
11. Blaettler, L., Mertz, D., Frei, R., Elzi, L., Widmer, A. F., Battegay, M., and Fluckiger, U. (2009) Secular trend and risk factors for antimicrobial resistance in Escherichia coli isolates in Switzerland 1997-2007. *Infection* 37, 534-539
12. Kobir, A., Shi, L., Boskovic, A., Grangeasse, C., Franjevic, D., and Mijakovic, I. (2011) Protein phosphorylation in bacterial signal transduction. *Biochimica et biophysica acta* 1810, 989-994
13. Kalantari, A., Derouiche, A., Shi, L., and Mijakovic, I. (2015) Serine/threonine/tyrosine phosphorylation regulates DNA binding of bacterial transcriptional regulators. *Microbiology* 161, 1720-1729
14. Tiwari, S., Jamal, S. B., Hassan, S. S., Carvalho, P., Almeida, S., Barh, D., Ghosh, P., Silva, A., Castro, T. L. P., and Azevedo, V. (2017) Two-Component Signal Transduction Systems of Pathogenic Bacteria As Targets for Antimicrobial Therapy: An Overview. *Frontiers in microbiology* 8, 1878
15. Pensinger, D. A., Schaenzer, A. J., and Sauer, J. D. (2018) Do Shoot the Messenger: PASTA Kinases as Virulence Determinants and Antibiotic Targets. *Trends Microbiol* 26, 56-69
16. Potel, C. M., Lin, M. H., Heck, A. J. R., and Lemeer, S. (2018) Widespread bacterial protein histidine phosphorylation revealed by mass spectrometry-based proteomics. *Nat Methods* 15, 187-190
17. Potel, C. M., Lin, M. H., Heck, A. J. R., and Lemeer, S. (2018) Defeating Major Contaminants in Fe(3+)- Immobilized Metal Ion Affinity Chromatography (IMAC) Phosphopeptide Enrichment. *Mol Cell Proteomics* 17, 1028-1034

18. Hengzhuang, W., Wu, H., Ciofu, O., Song, Z., and Hoiby, N. (2011) Pharmacokinetics/pharmacodynamics of colistin and imipenem on mucoid and nonmucoid Pseudomonas aeruginosa biofilms. *Antimicrob Agents Chemother* 55, 4469-4474
19. Cox, J., and Mann, M. (2008) MaxQuant enables high peptide identification rates, individualized p.p.b.-range mass accuracies and proteome-wide protein quantification. *Nature biotechnology* 26, 1367-1372
20. Tyanova, S., Temu, T., Sinitcyn, P., Carlson, A., Hein, M. Y., Geiger, T., Mann, M., and Cox, J. (2016) The Perseus computational platform for comprehensive analysis of (prote)omics data. *Nat Methods* 13, 731-740
21. Bindea, G., Mlecnik, B., Hackl, H., Charoentong, P., Tosolini, M., Kirilovsky, A., Fridman, W. H., Pages, F., Trajanoski, Z., and Galon, J. (2009) ClueGO: a Cytoscape plug-in to decipher functionally grouped gene ontology and pathway annotation networks. *Bioinformatics* 25, 1091-1093
22. Schwartz, D., and Gygi, S. P. (2005) An iterative statistical approach to the identification of protein phosphorylation motifs from large-scale data sets. *Nature biotechnology* 23, 1391-1398
23. Colaert, N., Helsens, K., Martens, L., Vandekerckhove, J., and Gevaert, K. (2009) Improved visualization of protein consensus sequences by iceLogo. *Nat Methods* 6, 786-787
24. Soufi, B., Krug, K., Harst, A., and Macek, B. (2015) Characterization of the E. coli proteome and its modifications during growth and ethanol stress. *Frontiers in microbiology* 6, 103
25. Knowles, T. J., Scott-Tucker, A., Overduin, M., and Henderson, I. R. (2009) Membrane protein architects: the role of the BAM complex in outer membrane protein assembly. *Nat Rev Microbiol* 7, 206-214
26. Gu, Y., Stansfeld, P. J., Zeng, Y., Dong, H., Wang, W., and Dong, C. (2015) Lipopolysaccharide is inserted into the outer membrane through an intramembrane hole, a lumen gate, and the lateral opening of LptD. *Structure* 23, 496-504
27. Cavallari, J. F., Lamers, R. P., Scheurwater, E. M., Matos, A. L., and Burrows, L. L. (2013) Changes to its peptidoglycan-remodeling enzyme repertoire modulate beta-lactam resistance in Pseudomonas aeruginosa. *Antimicrob Agents Chemother* 57, 3078-3084
28. Handel, N., Schuurmans, J. M., Brul, S., and ter Kuile, B. H. (2013) Compensation of the metabolic costs of antibiotic resistance by physiological adaptation in Escherichia coli. *Antimicrob Agents Chemother* 57, 3752-3762
29. Zampieri, M., Enke, T., Chubukov, V., Ricci, V., Piddock, L., and Sauer, U. (2017) Metabolic constraints on the evolution of antibiotic resistance. *Mol Syst Biol* 13, 917
30. Mijakovic, I., and Macek, B. (2012) Impact of phosphoproteomics on studies of bacterial physiology. *FEMS Microbiol Rev* 36, 877-892
31. Soares, N. C., Spat, P., Krug, K., and Macek, B. (2013) Global dynamics of the Escherichia coli proteome and phosphoproteome during growth in minimal medium. *J Proteome Res* 12, 2611-2621
32. Sharma, K., D'Souza, R. C., Tyanova, S., Schaab, C., Wisniewski, J. R., Cox, J., and Mann, M. (2014) Ultradeep human phosphoproteome reveals a distinct regulatory nature of Tyr and Ser/Thr-based signaling. *Cell reports* 8, 1583-1594
33. Lin, M. H., Sugiyama, N., and Ishihama, Y. (2015) Systematic profiling of the bacterial phosphoproteome reveals bacterium-specific features of phosphorylation. *Sci Signal* 8, rs10
34. Pan, Z., Wang, B., Zhang, Y., Wang, Y., Ullah, S., Jian, R., Liu, Z., and Xue, Y. (2015) dbPSP: a curated database for protein phosphorylation sites in prokaryotes. *Database (Oxford)* 2015, bav031
35. Loui, C., Chang, A. C., and Lu, S. (2009) Role of the ArcAB two-component system in the resistance of Escherichia coli to reactive oxygen stress. *BMC microbiology* 9, 183
36. Yu, Z., Zhu, Y., Qin, W., Yin, J., and Qiu, J. (2017) Oxidative Stress Induced by Polymyxin E Is Involved in Rapid Killing of Paenibacillus polymyxa. *BioMed research international* 2017, 5437139
37. Frost, L. S., and Koraimann, G. (2010) Regulation of bacterial conjugation: balancing opportunity with adversity. *Future Microbiol* 5, 1057-1071

38. Nachin, L., Nannmark, U., and Nystrom, T. (2005) Differential roles of the universal stress proteins of Escherichia coli in oxidative stress resistance, adhesion, and motility. *Journal of bacteriology* 187, 6265-6272
39. Vega, N. M., Allison, K. R., Khalil, A. S., and Collins, J. J. (2012) Signaling-mediated bacterial persister formation. *Nature chemical biology* 8, 431-433
40. Li, H., Wang, B. C., Xu, W. J., Lin, X. M., and Peng, X. X. (2008) Identification and network of outer membrane proteins regulating streptomysin resistance in Escherichia coli. *J Proteome Res* 7, 4040-4049
41. Moussatova, A., Kandt, C., O'Mara, M. L., and Tieleman, D. P. (2008) ATP-binding cassette transporters in Escherichia coli. *Biochimica et biophysica acta* 1778, 1757-1771
42. Correia, F. F., D'Onofrio, A., Rejtar, T., Li, L., Karger, B. L., Makarova, K., Koonin, E. V., and Lewis, K. (2006) Kinase activity of overexpressed HipA is required for growth arrest and multidrug tolerance in Escherichia coli. *Journal of bacteriology* 188, 8360-8367
43. Erickson, K. D., and Detweiler, C. S. (2006) The Rcs phosphorelay system is specific to enteric pathogens/commensals and activates ydeI, a gene important for persistent Salmonella infection of mice. *Molecular microbiology* 62, 883-894
44. Nishino, K., and Yamaguchi, A. (2004) Role of histone-like protein H-NS in multidrug resistance of Escherichia coli. *Journal of bacteriology* 186, 1423-1429
45. Shiraishi, K., Ogata, Y., Hanada, K., Kano, Y., and Ikeda, H. (2007) Roles of the DNA binding proteins H-NS and StpA in homologous recombination and repair of bleomycin-induced damage in Escherichia coli. *Genes & genetic systems* 82, 433-439
46. Deighan, P., Free, A., and Dorman, C. J. (2000) A role for the Escherichia coli H-NS-like protein StpA in OmpF porin expression through modulation of micF RNA stability. *Molecular microbiology* 38, 126-139
47. Sawicka, A., and Seiser, C. (2014) Sensing core histone phosphorylation - a matter of perfect timing. *Biochimica et biophysica acta* 1839, 711-718
48. Wright, D. P., and Ulijasz, A. T. (2014) Regulation of transcription by eukaryotic-like serine-threonine kinases and phosphatases in Gram-positive bacterial pathogens. *Virulence* 5, 863-885

Figure 1

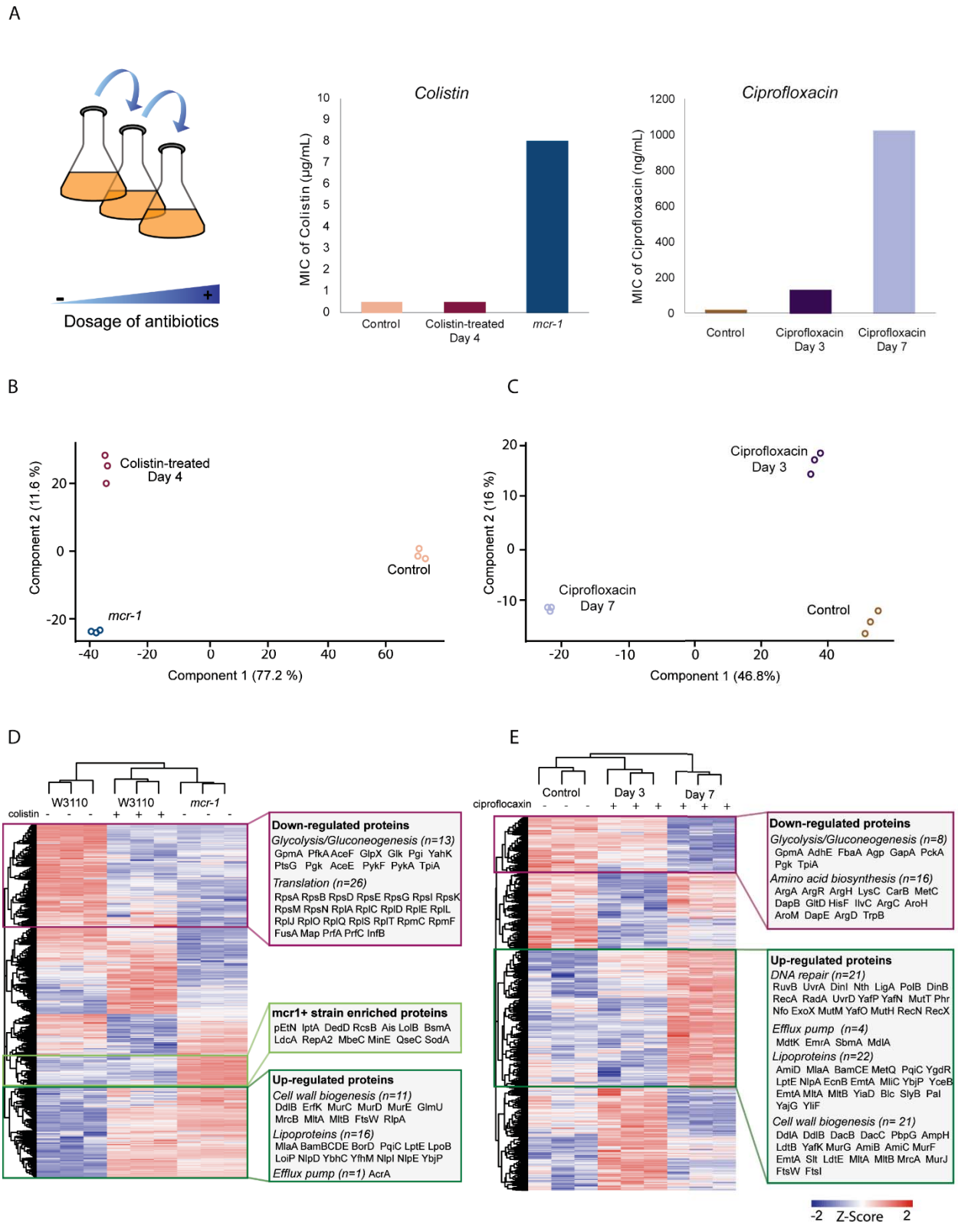

Figure 1. Quantitative proteomic analysis of *E.coli* continuously exposed to colistin or ciprofloxacin. (A) Wild-type *E. coli* cells were continuously exposed to the antibiotics colistin or ciprofloxacin with the concentration being one quarter of the MIC. No MIC increase was noticed after 4 days of exposure to colistin, while the clinically isolated *mcr-1* strain exhibited a MIC of 8 μg/mL. However, after 3 and 7 days of exposure to ciprofloxacin, the MIC increased 8-fold (128 ng/mL) and 64-fold (1024 ng/mL), respectively. (B, C) Principle component analysis shows that the three replicates cluster together, indicating good reproducibility. (B) Pink circles represent the control wild-type *E. coli* W3110 strain without colistin treatment. The purple circles represent the 4 days colistin treated *E. coli* cells, blue circles represent the *mcr-1 E. coli* strain. This analysis of protein expression patterns clearly showed that colistin treated *E. coli* cells were closer to the *mcr-1* strain. (C) Purple and violet circles are representing *E. coli* cells harvested after 3 days or 7 days of ciprofloxacin treatment, respectively and brown circles represent the non-treated control. For ciprofloxacin, *E. coli* cells with an induced higher MIC (day 3, day 7) showed different patterns compared to non-treated *E. coli* cells. (D, E) Unsupervised clustering analysis of the changes in the proteome following induction of resistance to (D) colistin and (E) ciproflxacin. The color code shows the relative abundance based on the Z-score. On the right, for each box that is highlighted in the cluster analysis, the enriched pathways are displayed. Proteins that belong to a specific cluster and participate in a certain pathway are indicated by their gene names. The pathway enrichment was performed using PANTHER (p-values <0.05).

Figure 2

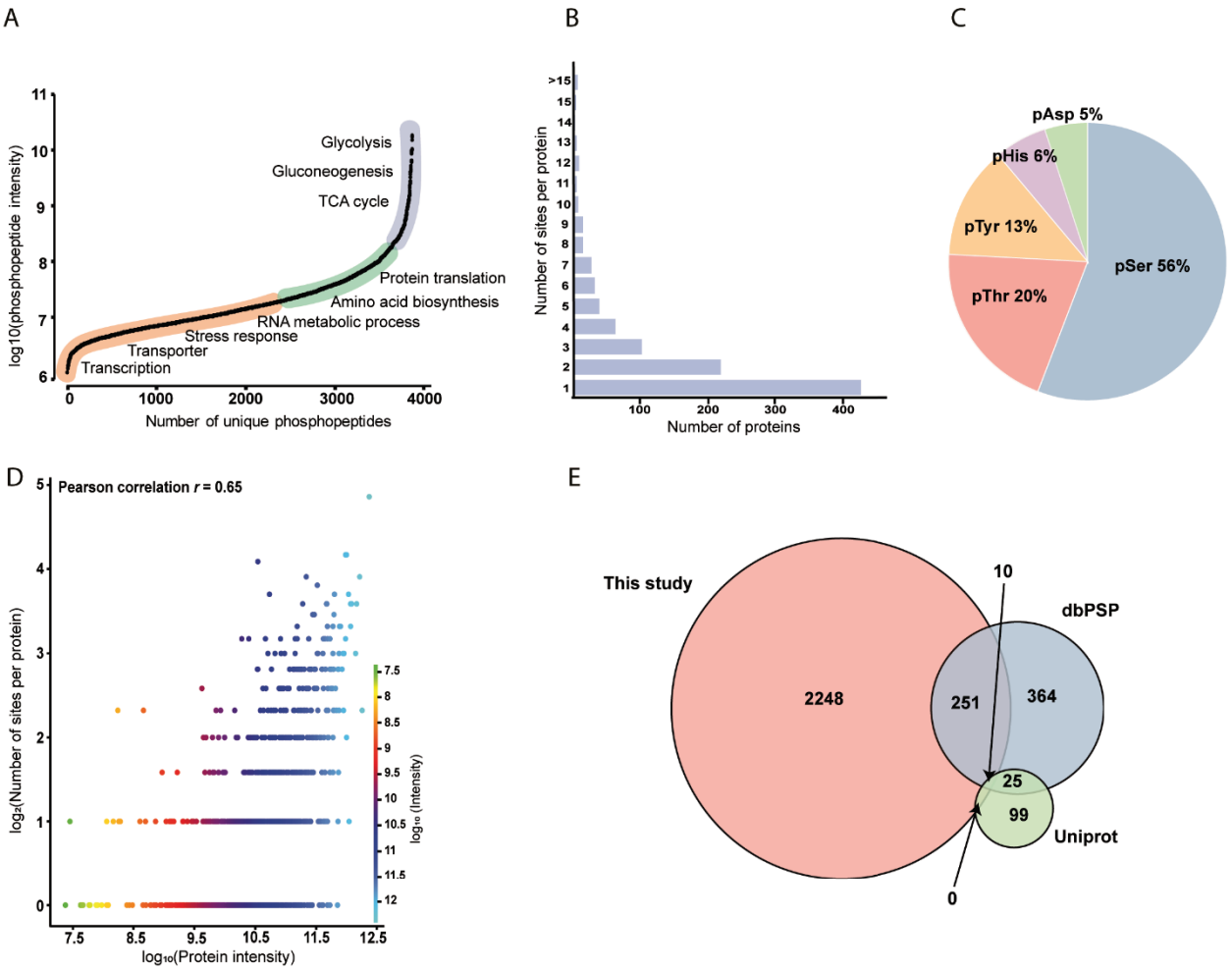

Figure 2. Comprehensive profiling of the *E. coli* phosphoproteome. (A) Dynamic range of the quantifiable phosphopeptides with the corresponding overrepresented biological process GO terms. GO term enrichment was performed using PANTHER (http://www.pantherdb.org/) with p-value < 0.05. (B) Correlation between the number of phosphosites per protein and protein abundance shows there is a weak correlation (Pearson correlation is 0.65). The color code indicates the protein abundance at $\log_{10}$ scale. (C) Characterization of the phosphoproteins based on the number of phosphosites indicated that most of the proteins, around 45%, only have one phosphosite. (D) Phosphosite distribution across S/T/Y/H/D residues. (E) The overlap between phosphosites identified in this study and public databases, dbPSP and Uniprot, showing the up to 89.6% of phosphosites identified in this study are novel phosphosites.

Figure 3

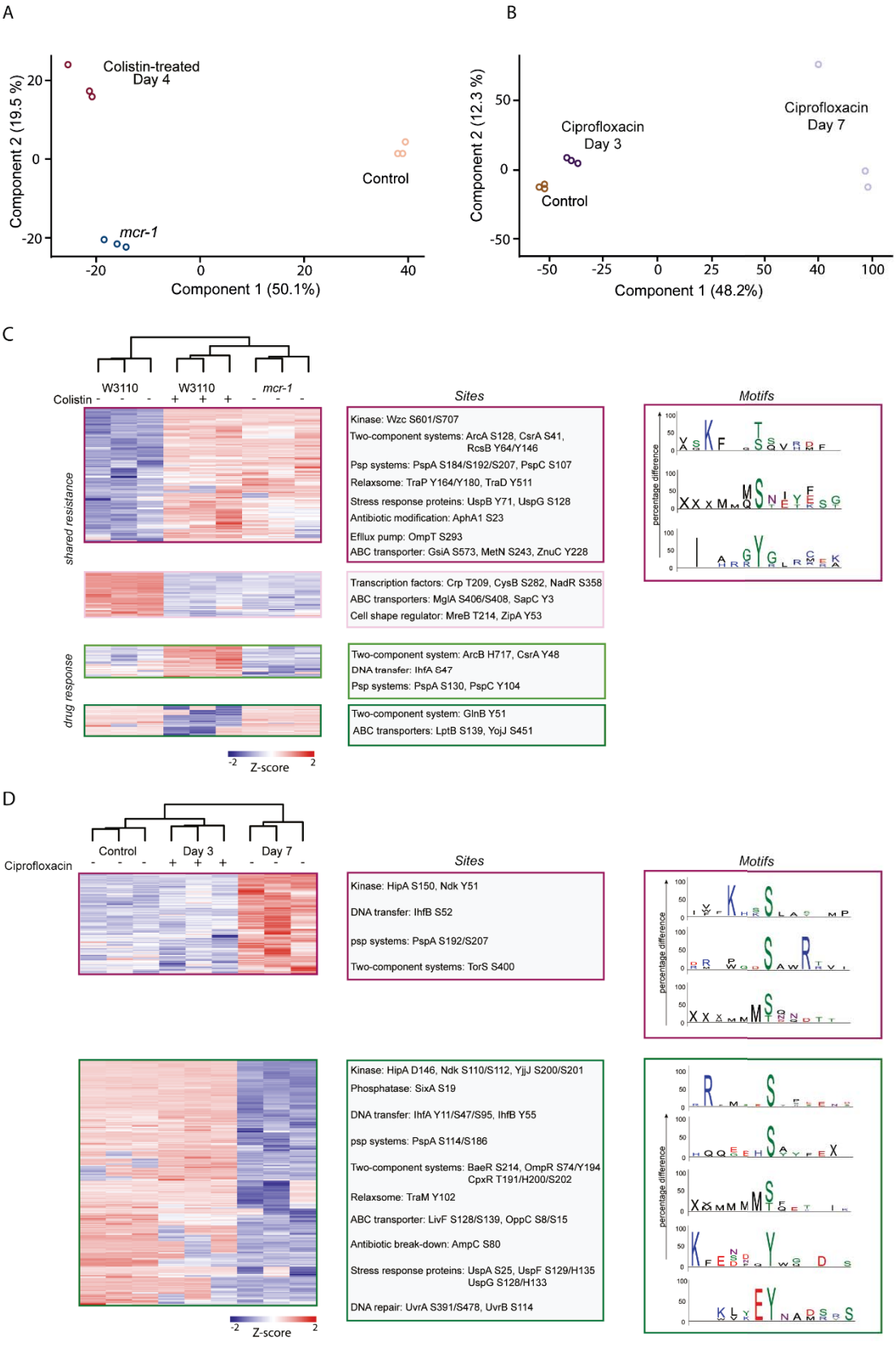

Figure 3. Phosphoproteomes of *E. coli* changes extensively upon colistin and ciprofloxacin treatment. As observed for the proteome analysis, triplicate phosphoproteomics samples clustered well together. (A) The pink circles represent the control *E. coli* W3110 strain without colistin treatment, whereas purple circles represent data from the serially-passaged wile-type *E.coli* cells treated with colistin. Blue circles represent data from the *mcr-1 E. coli* strain. Colistin-treated wild-type *E. coli* cells are in this analysis closer to the *mcr-1* strain, suggesting that common resistance mechanisms are partially shared. (B) For ciprofloxacin treatment, brown circles represent the control wild-type *E. coli* W3110 strain without ciprofloxacin treatment and purple and violet circles are representing the *E. coli* cells harvested after 3 days or 7 days treatment with ciprofloxacin, respectively. (C, D) Heatmap clustering of phosphorylation profiles after (C) colistin and (D) ciprofloxacin treatment. Each box represents a distinct unsupervised cluster profile across the different antibiotic susceptibilities. The color scale from blue to red indicates the Z-score, indicating decreased and increased phosphorylation. Regulated phosphosites in known resistance-related pathways are shown in the middle. Enriched phosphorylation motifs within particular clusters are displayed on the right, implicating that some specific kinases are involved in regulation. X was used to represent the N- or C-terminal position but not any particular amino acid. N-terminal phosphorylation was overrepresented in both treatments, while the C-terminal phosphorylation is only regulated in ciprofloxacin treatment. Three tyrosine phosphorylation motifs were enriched as well as four basophilic motifs.

Figure 4

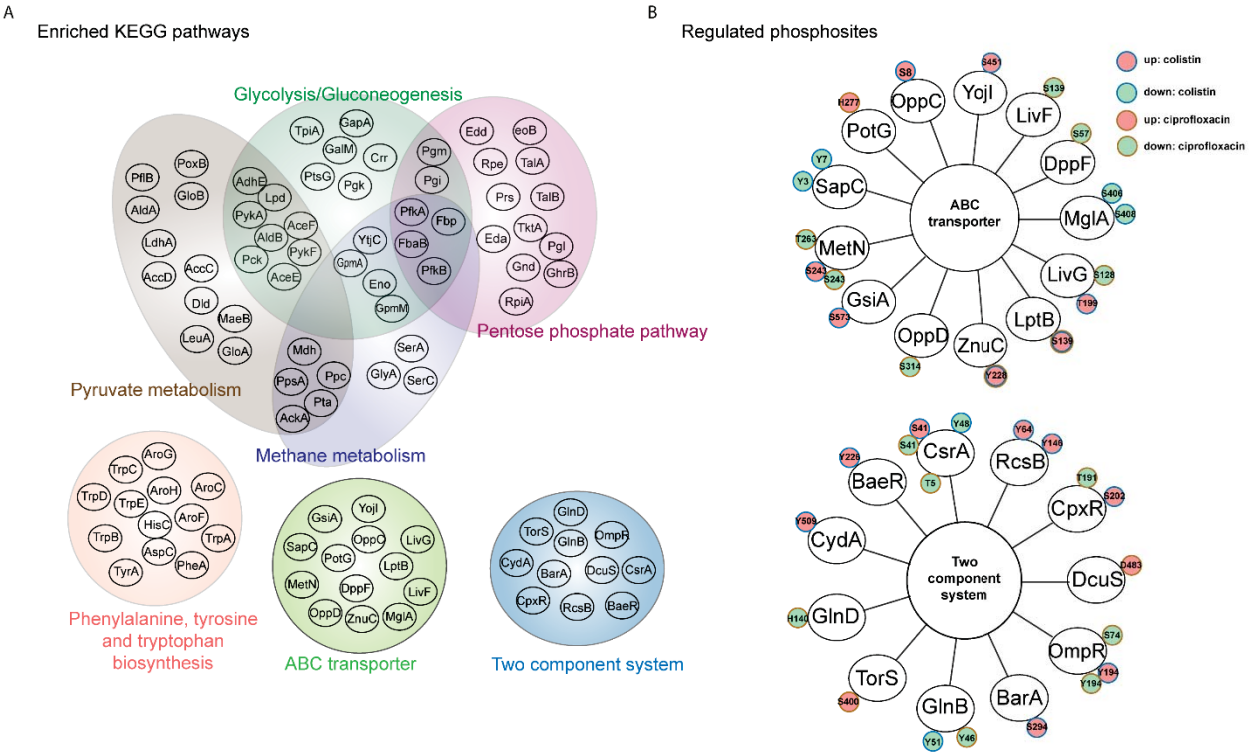

Figure 4. KEGG pathway enrichment analysis based on regulated phosphosites containing proteins from both colistin and ciprofloxacin treatments. (A) In total, 555 phosphoproteins were subjected to KEGG pathway enrichment using Cytoscape with the ClueGO app. The pathways shown here are significantly enriched with p-value < 0.05. Black circles represent the phosphoproteins containing regulated phosphosites, while the colored ellipses represent each overrepresented pathways. Proteins inside overlapping pathways indicate that these proteins are involved in multiple pathways. (B) The regulated phosphosites identified in ABC transporter and two component system upon colistin (blue circle) and ciprofloxacin (brown circle) treatments (green :downregulated, pink: upregulated).

Figure 5

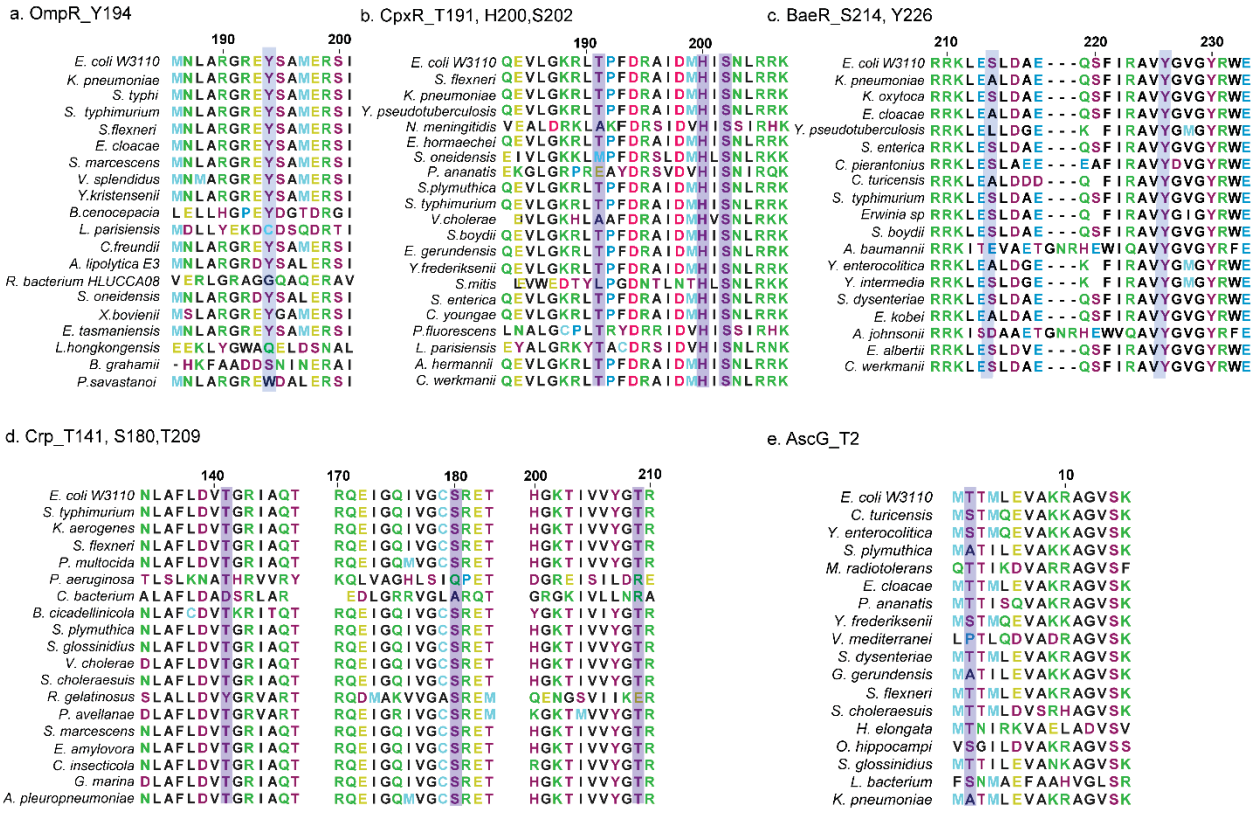

Figure 5. Observed phosphosites are highly conserved on the helix-turn-helix regions of several transcription factors as revealed by sequence alignment across different bacteria. (A-C) Alignment of regulated phosphosites in the OmpR/PhoB subfamily transcription factors, including the Y194 on OmpR, H200 and S202 on CpxR, and S214 and Y226 on BaeR. (D, E) Alignment of phosphorylated residues on the non-OmpR/PhoB subfamily transcription factors, which are T141, S180, and T209 on Crp and T2 on AscG. These phosphosites have high conservation across different bacteria indicating a possible conserved role in regulations. Sequence alignment was performed with Clustal X with default parameters. The purple boxes represent the phosphosites identified in this study.

Figure 6

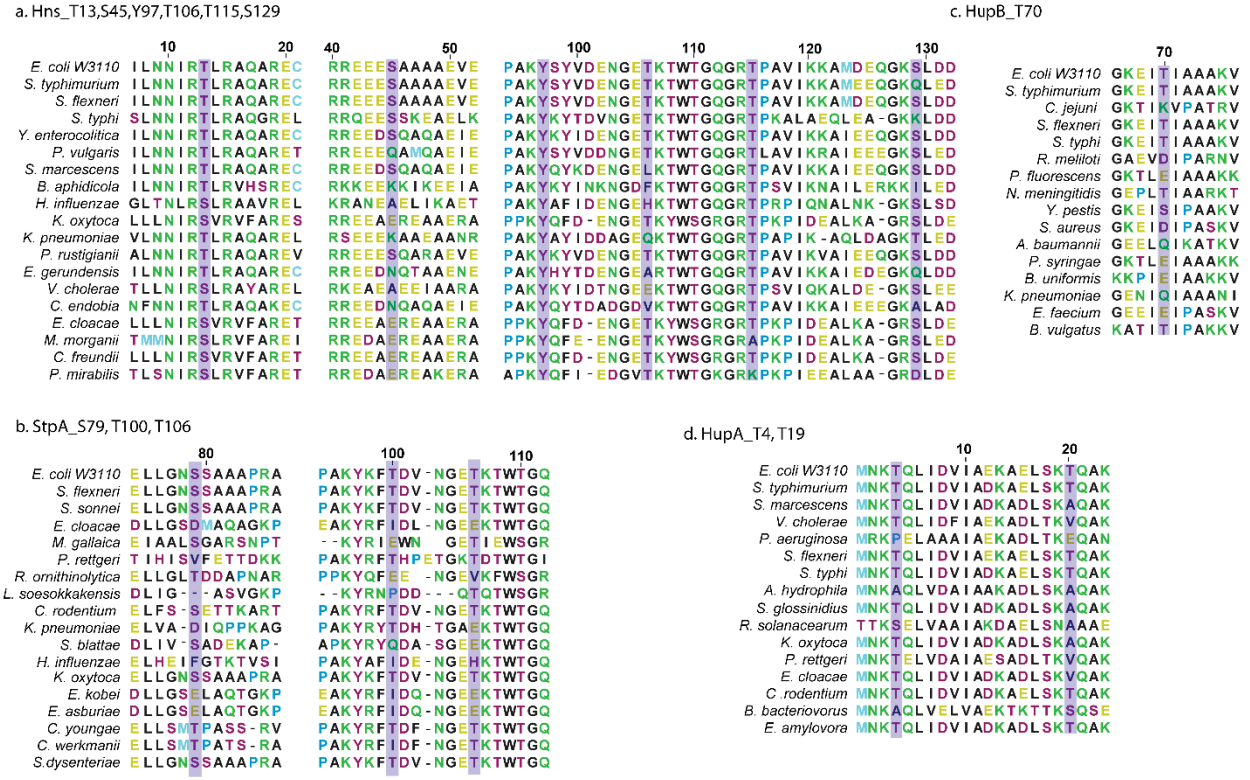

Figure 6. Observed phosphosites are highly conserved in a variety of DNA binding proteins across different bacteria. The phosphosites identified on DNA binding proteins (in purple boxes) include (A) T13, S45, Y97, T106, T115 and S129 on Hns, (B) S79, T100, and T106 on StpA, (C) T70 on HupB, and (d) T4 and T19 on HupA. Although S45 on Hns and T70 on HupB display slightly lower conservation, the high prevalence of acidic amino acids instead of Ser or Thr may reflect the fact that the negative charge is essential for protein functions.